Science of the Total Environment 963 (2025) 178486

Contents lists available at ScienceDirect

Science of the Total Environment

journal homepage: www.elsevier.com/locate/scitotenv

Unraveling the shifts in the belowground microbiota and metabolome of *Pinus pinaster* trees affected by forest decline

Ana V. Lasa [a], Miriam López-Hinojosa [b], Pablo J. Villadas [a], Antonio José Fernández-González [a], María Teresa Cervera [b], Manuel Fernández-López [a,*]

[a] *Microbiology of Agroforestry Ecosystems, Department of Soil and Plant Microbiology, Estación Experimental del Zaidín, CSIC, Profesor Albareda 1, 18008 Granada, Spain*

[b] *Forest Tree Genomics, Department of Forest Ecology and Genetics, Instituto de Ciencias Forestales, Instituto Nacional de Investigación y Tecnología Agraria y Alimentaria, CSIC (ICIFOR-INIA-CSIC), Carretera de La Coruña Km 7,5, 28040 Madrid, Spain*

HIGHLIGHTS

- Decline-affected and healthy pines harbor distinct root-associated microbiota.
- Microbial networks of diseased trees are less complex than that of healthy ones.
- Root endosphere of healthy trees was enriched in ectomycorrhizal fungi.
- Metabolic analysis revealed distinct profiles in healthy and decline-affected pines.
- The abundance of several metabolites and microorganisms were correlated.

GRAPHICAL ABSTRACT

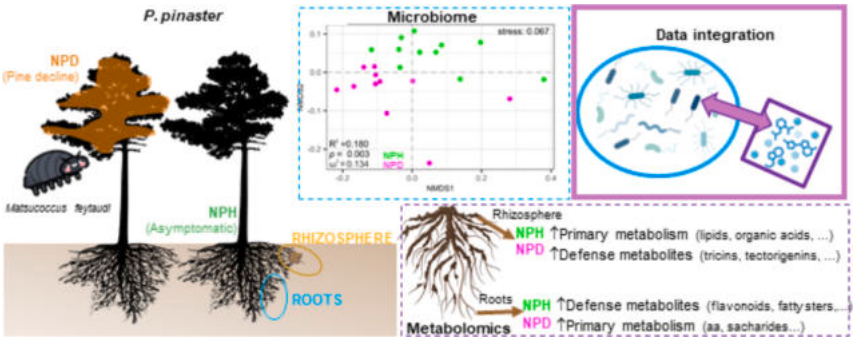

ARTICLE INFO

Editor: Charlotte Poschenrieder

Keywords:
Forest decay
Metabarcoding
Maritime pine
Cry-for-help
Root exudates
Metabolic profiles

ABSTRACT

Pinus pinaster Aiton (maritime pine) stands are suffering a generalized deterioration due to different decline episodes throughout all its distribution area. It is well known that external disturbances can alter the plant associated microbiota and metabolome, which ultimately can entail the disruption of the normal growth of the hosts. Notwithstanding, very little is known about the shifts in the microbiota and the metabolome in pine trees affected by decline. The aim of our work was to unravel whether bacterial and fungal communities inhabiting the rhizosphere and root endosphere of *P. pinaster* trees with symptoms of decline and affected by *Matsucoccus feytaudi* in the National Park of Sierra Nevada (Granada, Spain) showed alterations in the structure, taxonomical profiles and associative patterns. We also aimed at deciphering potential changes in the rhizosphere and root metabolome. Trees infected by *M. feytaudi* and healthy individual harbored distinct microbial communities at both compositional and associative patterns. Unhealthy trees were enriched selectively in certain plant growth promoting microorganisms such as several ectomycorrhizal fungi (*Clavulina*) and *Streptomyces*, while other beneficial microorganisms (*Micromonospora*) were more abundant in unaffected pines. The rhizosphere of unhealthy trees was richer in secondary metabolites involved in plant defense than healthy pines, while the opposite trend was detected in root samples. The abundance of certain microorganisms was significantly

* Corresponding author.
E-mail address: manuel.fernandez@eez.csic.es (M. Fernández-López).

https://doi.org/10.1016/j.scitotenv.2025.178486
Received 11 October 2024; Received in revised form 8 January 2025; Accepted 10 January 2025

correlated with several antimicrobial metabolites, thus, being all of them worthy of further isolation and study of their role in forest decline.

1. Introduction

Maritime pine (*Pinus pinaster* Aiton) is the second most widely distributed coniferous species in Spain (Spanish Ministry for Ecological Transition and the Demographic Challenge, 2024), being also widespread in other western Mediterranean countries such as Portugal, southern France, western Italy as well as fragmented populations in northern Morocco, Algeria and Tunisia. This species is well known for its adaptive response to droughts (de María et al., 2020; López-Hinojosa et al., 2021; López-Hidalgo et al., 2023; Manjarrez et al., 2024), which makes it an excellent candidate for conservation and afforestation tasks, especially in the Mediterranean basin, where an increase in the temperatures and drought intensity and frequency are expected (Ali et al., 2022). Despite that, a great decline of *P. pinaster* stands has been reported in the last decade in the Iberian Peninsula (Álvarez et al., 2015; Prieto-Recio et al., 2015; Gea-Izquierdo et al., 2019; Calama et al., 2024).

Tree decline is a complex phenomenon affecting our forests worldwide (Allen et al., 2010). It results in crown dieback (yellowing and defoliation) and reduced tree growth, which can lead to death. Although there is no consensus on the main cause of forest decline, it is widely accepted that it is a multifactorial phenomenon in which biotic and abiotic stressors interact each other (Manion, 1991; Coyle et al., 2015). Much work has been devoted to understand the contribution of abiotic factors, among which drought events are considered the main drivers of forest decline (Carnicer et al., 2011; Madrigal-González and Zavala, 2014; Calvão et al., 2019). In the case of *P. pinaster*, it has been demonstrated that certain pathogens and pests such as the insect *Matsucoccus feytaudi* are partially involved in decline episodes (Calvão et al., 2019; Gea-Izquierdo et al., 2019; Azcárate et al., 2023). Indeed, *M. feytaudi* was identified as the cause of maritime pines die-off episodes in 2017 in south France (120,000 ha affected) and decline episodes in the Natural Park of Sierra de Baza (2000 ha) and the National Park of Sierra Nevada, specifically, in Jérez del Marquesado (Granada, Spain) (Guzmán Álvarez et al., 2020).

Plant-associated microorganisms are considered the first line of defense of their host as many of them are able to suppress plant pathogens, stimulate the host defense system, and deploy plant growth promoting abilities (Mannaa and Seo, 2021). As a result of an external disturbance (biotic and/or abiotic stress), plants can alter the composition of the root exudates and recruit specific microorganisms which aid in coping with this stressor. The specific metabolites that attract beneficial microorganisms depend on the plant host, but what is common in many cases is that this microorganism-mediated response involves a change in the structure of the plant-associated microbial communities (Seybold et al., 2020). Thus, recent works are considering plant diseases from a holistic perspective, integrating data of plant physiology, genomics, metabolomics (Dove et al., 2022) and its associated microbiota (Fernández-González et al., 2020; Trivedi et al., 2020).

In the case of pine decline episodes, Proença et al. (2017) gave evidence for significant shifts in the structure of wood endophytic bacteria of *P. pinaster* trees infected by the pine nematode (*Bursaphelenchus xylophilus*), and Lasa et al. (2024) uncovered the differences in the root microbiota of decline-affected and unaffected *P. sylvestris* trees. Concurrently, López-Hidalgo et al. (2023) deciphered distinct metabolic profiles when *P. pinaster* trees were subjected to different intensities of heat and drought stresses, while Riquelme et al. (2023) registered the metabolic shifts in *P. radiata* individuals as a consequence of the infection by the pathogenic wasp *Sirex noctilio*. Nevertheless, the knowledge about the metabolome of decline-affected pines is still fragmentary, and there are no works coupling the microbiota and metabolomics data in conifers. Hence, we aimed at unraveling the shifts in microbiome and metabolome of the rhizosphere and root endosphere of *P. pinaster* trees affected by forest decline and infected by the insect *Matsucoccus feytaudi*, located at the Sierra Nevada National Park (Granada, southeast Spain). Based on the microbiome and metabolome alterations reported previously as a consequence of biotic and abiotic stressors, we hypothesized that differences in microbiota and metabolic profiles between healthy and declining *P. pinaster* trees are coupled.

2. Material and methods

2.1. Experimental site

The experimental site is located in Jérez del Marquesado (Sierra Nevada National Park, Granada, Spain), covered by a *Pinus pinaster* forest. The coordinates and specific characteristics of the area under study are summarized in Table S1. 12 individuals of *P. pinaster* expressing symptoms of decline (yellowing of the crown, defoliation and/or reduced growth; NPD samples, *Sierra Nevada P. pinaster Decline*) were selected. Both sampling sites were <200 m apart (Fig. S1). It should be marked that NPD trees showed resin exudation and changes in bark consistency, due to the attack of *Matsucoccus feytaudi*. 12 trees of the same species with no symptoms of pine decline were chosen as control trees (NPH samples, *Sierra Nevada P. pinaster Healthy*). All of the selected trees were approximately of the same age.

2.2. Sample collection and processing

Rhizosphere soil and roots collection was performed in spring (April 25, 2022) in both cases, when the vegetative growth of the trees is intense. The collection of rhizosphere soil was carried out according to Lasa et al., 2022b. Briefly, the litter and topsoil were removed by digging (5–25 cm depth) in order to avoid the soil horizon rich in organic matter and the collection of the roots of herbaceous plants (Fig. S2). The main roots of the pines were followed until the young, non-suberified roots were found, which are the most metabolically active and those with the greatest water and nutrient absorption capability. In order to take samples representative of each tree, the soil firmly attached to the roots was taken from two points of the root system by rubbing them manually (2 g approximately). Roots were also collected at the same two points and maintained at 4 °C until they were processed in the laboratory (within 24 h). Thus, for each tree two samples of roots and rhizosphere soil were taken for microbiome analyses (2 × 24 trees). For metabolomics procedures, an additional sample of rhizosphere soil was collected per tree (1 g). In order to measure the physicochemical properties of the soil, an extra sample (500 g) was collected near the selected roots of each tree at the same moment. Edaphic properties were measured by Laboratorio Analítico Bioclínico (Almería, Spain) by standardized procedures.

Collected roots were surface sterilized as described by Fernández-González et al. (2020). In brief, roots were washed with NaCl 0.8 % (*w/v*) and immersed in an ethanol solution (70 %, *v*/v) and then in a NaClO solution (4 %, v/v) with Tween 20 (0.01 %, v/v). After rinsing the sterilized roots with sterile distilled water, they were stored at −80 °C. Roots were subsequently lyophilized at −45 °C (72 h) by means of the freeze dryer Thermo Savant Modulyo D-230 (Waltham, MA, United States) and ground in the grinder MM-400 (Retsch, Haan, Germany) with the help of one sterilized grinding ball (20 mm diameter), at 30 Hz for 1 min. Obtained root material was immediately processed.

2.3. DNA extraction and sequencing

0.25 g and 0.1 g of rhizosphere soil and lyophilized root samples were used for DNA extraction, respectively. For that purpose, DNeasy® PowerSoil® Pro and DNeasy® Plant Pro Kits (Qiagen; Hilden, Germany) were employed, respectively, according to manufacturers' instructions. For both plant compartments (rhizosphere soil and root endosphere), DNA extracted from the same tree was mixed into a composite sample (Fig. S2). DNA yields were quantified by means of the fluorimeter Qubit 3.0 (Life Technologies; Carlsbad, CA, United States).

DNA from each individual sample was sequenced by MiSeq Illumina platform at the Genomics Service of the Institute of Parasitology and Biomedicine López-Neyra (Granada, Spain). In particular, a 2 × 275 PE strategy was followed. The V3-V4 hypervariable regions of the bacterial *16S rRNA* gene were sequenced by using the primer pair Pro341F and Pro805R (Takahashi et al., 2014), while primers ITS4 (White et al., 1990) and fITS7 (Ihrmark et al., 2012) were employed to amplify the fungal ITS2 region. In the case of root endosphere libraries, V3-V4 amplicons were treated with PNA PCR clamps in order to diminish the amplification of plastids and mitochondrial sequences (Lundberg et al., 2013). In each sequencing run, three replicates of the mock-community ZymoBIOMICS Microbial Community Standard II (logarithmic distribution; ZYMO Research, Irvine, CA, United States) were included as sequencing controls.

2.4. Illumina data processing

All data processing was performed in R software v 4.2.3 (R Core Team, 2022) using the package DADA2 and its corresponding functions (Callahan et al., 2016) unless otherwise stated. Bacterial and fungal reads were processed in the same way except where indicated. After checking the quality of forward and reverse raw reads, Figaro bioinformatic tool (Sasada et al., 2020) was implemented just for the bacterial dataset, in order to infer the best parameters for the subsequent trimming of the reads. A quality filtering step was carried out in which bacterial reads with ambiguities, shorter than 50 bp, and with higher expected errors than those proposed by Figaro were discarded from the analysis (*filterAndTrim* function). Then, both bacterial and fungal primers were removed from the reads by running cutadapt tool (Martin, 2011). In the case of fungal libraries, the filtering and trimming step was performed after the removal of primers. For both bacterial and fungal data, error rates were learnt by running the function *learnErrors* and subsequently forward and reverse reads were overlapped by means of the function *mergePairs* and default parameters. Obtained sequences were grouped into Amplicon Sequence Variants (ASVs) and chimeras were removed from the datasets (function *removeBimeraDenovo*). The resulting quality sequences were taxonomically classified by comparing them to those held in the Ribosomal Database Project training set v.18 (RDP-II, Cole et al., 2014) and UNITE v. 7.2 (Abarenkov et al., 2022) for bacterial and fungal libraries, respectively. We calculated the relative abundance of the most abundant ASV detected in the samples corresponding to the mock community but which are not part of the commercial community included in the sequencing run (0.00597 % of the total reads). Thus, ASVs below this detection limit were considered sequencing artifact and removed from the analyses. ASVs classified as mitochondria, chloroplasts, unknown at kingdom level or Eukaryota (in the case of bacterial dataset) were not retained for further analyses.

2.5. Metabolomics procedures

Sample preparation, metabolomics analysis, compound identification and initial bioinformatics analyses were performed at oloBion company (Barcelona, Spain).

The soil and roots samples (0.25 g) were mixed independently with 1 mL of cold MeOH:H_2O (80:20) and 0.1 % formic acid solutions containing a mixture of internal standards, and then this mixture was homogenized with TissueLyzer II (Qiagen, Germany) for 5 min at 30 Hz with a steel bead. Then, the mixtures were centrifuged 5 min at 14000 rpm and filtered through 0.2 μm RC filters (Phenomenex, Spain) and characterized by high-resolution mass spectrometry, using a 1290 Infinity II ultra-high performance liquid chromatograph coupled to a 6560 Ion Mobility Q-TOF mass spectrometer (Agilent Technologies, CA, USA). The extracts were separated at 45 °C on a Water Acquity UPLC BEH C18 column (100 mm length x 2.1 mm id; 1.7 μm particle size) equipped with an additional Water Acquity VanGuard BEH C18 pre-column (5 mm × 2.1 mm id; 1.7 μm particle size) using (A) water with 0.1 % formic acid and (B) acetonitrile with 0.1 % formic acid as A and B mobile phases respectively. Compound identification was achieved using oloMAP (v1.0), a proprietary software that combines standard library MSMS identification and retention time prediction using Retip (Bonini et al., 2020).

2.6. Analysis of microbial communities

All the analyses regarding microbiota datasets were performed in R software v 4.2.3 by employing the packages and functions indicated below.

2.6.1. Rarefaction curves and alpha diversity

The function *rarecurve* included in the package vegan (Oksanen et al., 2022) was employed to compute the rarefaction curves. Data were rarefied to the smallest library size (function *rarefy_even_depth*, package phyloseq; McMurdie and Holmes, 2013) prior to alpha indices calculation (function *estimate_richness* (package phyloseq) to avoid the biases associated to different library size.

2.6.2. Beta diversity analyses

Hereinafter, all the analyses were performed based on non-rarefied dataset, as recommended McMurdie and Holmes (2014). Bacterial and fungal ASV counts were normalized by the Trimmed Means of M-value approach by applying the functions *DGEList* and *calcNormFactors* of the package edgeR (Robinson et al., 2010). Once normalized, Non-Metric Multidimensional Scaling (NMDS) analyses were carried out based on Weighted UniFrac distance and Bray-Curtis dissimilarity for bacterial and fungal communities, respectively (function *ordinate*, package phyloseq). PERMDISP2 test was applied (function *betadisper*; package vegan) to test the homogeneity of variances of the two groups of samples. Differences in the structure of the microbial communities between groups of samples were calculated by Permutational Analysis of Variance (PERMANOVA) by running the function *adonis2* (package vegan). The effect size of the differences was calculated by means of the function *Adonis_OmegaSq* (package MicEco; Russel, 2023).

2.6.3. Comparison of taxonomic profiles

In order to compare the abundance of each microbial taxon between symptomatic and non-affected trees, the Analysis of Compositions of Microbes with Bias Correction (ANCOM-BC; Lin and Peddada, 2020) was applied by implementing the function *ancombc2* of the package ANCOMBC developed by the abovementioned authors. Just taxa that were present in at least 90 % of the samples were kept for the analysis, setting the default parameters of the function.

2.6.4. Co-occurrence network construction and analysis

Microbial networks were calculated as described by Lasa et al. (2024) by using the Molecular Ecological Network Analysis Pipeline (MENAP) software (http://ieg4.rccc.ou.edu/mena/main.cgi). One network was constructed per plant compartment (rhizosphere, root endosphere) and per health status of the trees (NPD, NPH). In brief, ASV counts were centered log-transformed and similarity matrices based on Pearson (rhizosphere) and Spearman (endosphere) correlation coefficients were constructed. Indirect interactions among ASVs were not taken into account, and module calculation was then performed. The

topological values of the co-occurrence networks were compared each other after a randomization step in which 100 random networks with the same number of nodes and edges as each empirical network were constructed. For pairwise comparisons, the standard deviation of the random networks was considered and Student's *t*-tests were employed. Microbial ASVs were classified into peripherals, connectors, module and network hubs according to Olesen et al. (2017).

For metabolite-ASV co-occurrence networks, the same software and procedure as for microbe-microbiome co-occurrence network construction was applied, although some modifications were made. In this case, just differentially abundant metabolites were included in the analyses, and one network per plant compartment was calculated, thus, joining NPD and NPH-significantly enriched metabolites in the same network. Only those ASVs and metabolites detected in at least 50 % of the replicates of each group of samples were taken into account. Centered log-ratio transformation was applied to ASV and metabolite counts, as recommended by the developers for compositional datasets. For similarity matrices calculation, Spearman correlation coefficient was selected, and indirect interactions were removed from the analyses.

For the plotting of microbiome-microbiome and microbiome-metabolome co-occurrence networks the software Cytoscape v.3.7.2 (Shannon et al., 2003) was employed.

2.7. Metabolomics analysis

The analyses of the obtained data were conducted using the open-source software MetaboAnalyst 6.0 (Chong et al., 2018). Raw data underwent logarithmic transformation and Pareto scaling before being subjected to univariate analyses. Fold Change (FC) analysis was performed and combined with the results of univariate tests in volcano plots to select significant features based on both biological and statistical significance simultaneously, using a FC threshold of 1.5 and setting a threshold of q-value <0.05 from FDR (False Discovery Rate) correction. Heatmaps based on correlations along with a hierarchical clustering dendrogram employing the Euclidean distance measure and the Ward clustering algorithm were constructed. Furthermore, hierarchical clustering heatmaps were conducted to identify and compare differentially accumulated metabolites with unusually high/low values. In these analyses, the Euclidean distance measure and Ward clustering method were applied, focusing on the top 50 significantly different metabolites.

2.8. Univariate statistical analyses

All the univariate statistical tests were calculated in R software, by means of the functions included in the package rstatix (Kassambara, 2022) unless otherwise stated. Firstly, the assumption of normality and homoscedasticity was checked by means of Shapiro-Wilks and Levene tests, respectively (functions *shapiro_test* and *levene_test*). The presence of extreme outliers was addressed by the function *identify.outliers*.

In case of parametric data, the corresponding variables were compared between asymptomatic and affected trees by means of Student's *t*-test by applying the function *t-test*. When extreme outliers were found, two-sample Yuen robust t-test was applied after the trimming of 20 % of the total observations (function *YuenTTest*, package DescTools; Signorell et al., 2022). The effect size was measured by calculating Cohen's d and Yuen's ξ for parametric and trimmed data by using the functions *cohens_d* and *yuen.effect.ci* (package WRS2; Mair and Wilcox, 2020), respectively, and classified as described Cohen (1988). Correlations among metabolites were addressed by calculating Pearson's correlation coefficients. Confidence levels >95 % (α = 0.05) were selected for all the analyses.

3. Results

3.1. Edaphic parameters

Several physicochemical properties showed statistically significant differences between soils where healthy and affected trees were located. While NPH samples were significantly richer in organic matter and clay content and showed higher values of carbon to nitrogen ratio than NPD samples, the percentage of sand was significantly higher in the soil covered by unhealthy pines (Table S2).

3.2. General characteristic of the Illumina dataset

A total of 2,489,855 and 3,500,316 raw bacterial and fungal reads were retrieved from the Illumina platform, respectively, which resulted in 836,085 (bacteria) and 2,319,455 (fungi) quality sequences after the filtering and trimming steps (Table S3). Four and one samples were removed from the bacterial and fungal libraries, respectively, due to the low number of quality sequences registered or to an unusually low richness of the samples. The rhizosphere bacterial community was composed by 1866 and 2100 ASVs (NPH and NPD, respectively, while the dataset corresponding to root endosphere of healthy and affected trees comprised 743 and 617 bacterial ASVs, respectively. In the rhizosphere soil, 393 and 456 fungal ASVs (NPH and NPD, respectively) were registered, detecting 267 and 225 fungal ASVs in the root endosphere of symptomatic and asymptomatic pines, respectively. As shown in Fig. S3, the sequencing effort were enough since almost all the rarefaction curves reached to the asymptote.

3.3. Unraveling the differences in the diversity and structure of microbiota associated to the roots of healthy and decline-affected trees

Bacterial and fungal communities inhabiting the rhizosphere of symptomatic trees were significantly more diverse than that of healthy trees (Student' *t*-test, $p < 0.024$), and the former were also significantly evener (Yuen's t-test, $p = 0.003$). All these differences were classified as large, according to Cohen (1988; Table S4). On the other hand, the richness of the bacterial community inhabiting the root endosphere of healthy trees was higher than that of decline-affected pines (Student's t-test, $p = 0.046$, Cohen's d = 0.907), while no differences for any of the alpha indices analyzed were recorded for fungal endophytic populations.

When analyzing the structure of microbial communities, we observed that the dispersion of the two groups of samples was homogeneous for root endosphere bacteria and rhizosphere fungi (Table S5), while heteroscedasticity was detected for the samples corresponding to rhizosphere bacteria and endosphere fungal communities (PERMDISP2, $p^{\text{rhizosphere}}_{\text{bacteria}} = 0.022$; $p^{\text{endosphere}}_{\text{fungi}} = 0.045$). Notwithstanding, samples corresponding to rhizosphere bacteria and endosphere fungi of NPD and NPH pines were separated across the axis 1 of the NMDS (Fig. 1A and D), and statistically significant differences were registered in the structure of both populations (Fig. 1A and D). As shown in the NMDS plot (Fig. 1B), the structure of bacterial populations dwelling in the root endosphere of both types of trees differed to a small extent (PERMANOVA, $R^2 = 0.18$, $p = 0.003$, $\omega^2 = 0.134$).

Fungal communities dwelling in the root endosphere and rhizosphere soil showed significant differences in the structure when healthy and diseased trees where compared each other (Fig. 1C and D). In both cases, these differences were statistically significant albeit subtle (PERMANOVA, Rhizosphere: $R^2 = 0.16$, $p = 10^{-4}$, $\omega^2 = 0.12$; Root endosphere: $R^2 = 0.098$, $p = 10^{-4}$, $\omega^2 = 0.055$).

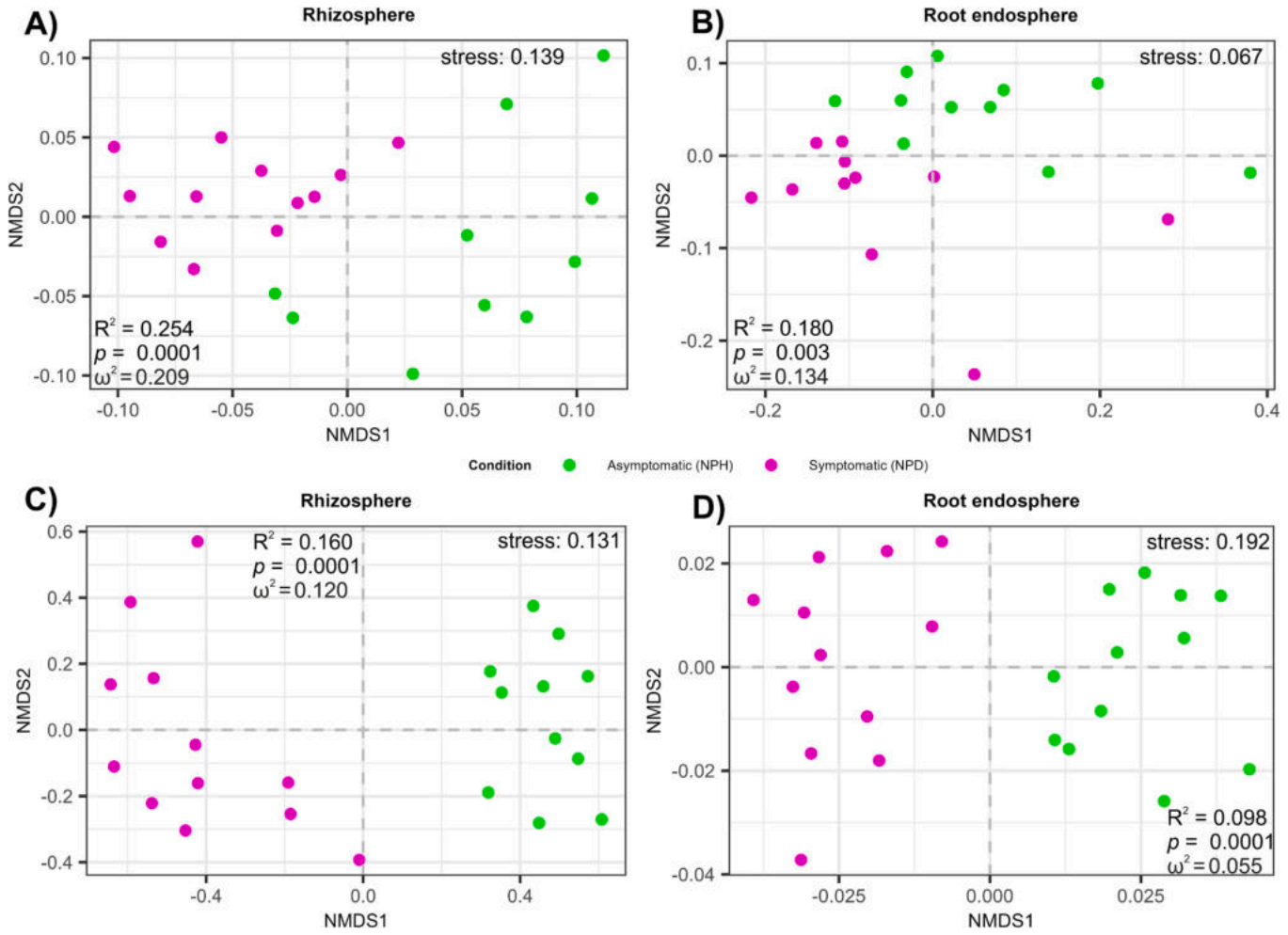

Fig. 1. Non-Metric Multidimensional Scaling (NMDS) of bacterial communities inhabiting the rhizosphere (A) and root endosphere (B), and fungal communities dwelling in the rhizosphere (C) and root endosphere (D) of healthy and decline-affected *P. pinaster* trees. NMDS of bacterial populations were calculated based on Weighted-UniFrac distances, while those of fungi were calculated based on Bray-Curtis dissimilarities.

3.4. Deciphering the changes in the taxonomical profiles of root-associated microbiota

Rhizosphere and root endosphere bacterial communities were comprised by 15 and 14 different phyla, respectively, although the latter were mainly dominated just by *Actinobacteria* and *Proteobacteria*, which accounted for >86 % of total sequences (Fig. S4A and B). In none of the cases archaeal sequences were detected. When NPD and NPH rhizosphere samples were compared to each other, significant differences were detected in the abundance of *Proteobacteria*, *Acidobacteria*, *Verrucomicrobia* and *Firmicutes*, and the last three phyla were enriched in the affected trees (Table S6). The root endosphere of decline-affected trees was significantly enriched in the phyla *Actinobacteria* and *Firmicutes*, being large the differences of the later phylum (Fig. S4B; ANCOM-BC, $p = 2.5 \cdot 10^{-6}$, W = 5.2).

Less taxonomical shifts were registered in the case of the mycobiome: among the most abundant phyla, just *Mortierellomycota* was significantly less represented in the rhizosphere of healthy trees (ANCOM-BC, $p = 7.74 \cdot 10^{-5}$, W = 4.42; Fig. S4C), whilst all the phyla were equally distributed in the root endosphere of both types of pines (ANCOM-BC, $p > 0.606$).

At genus level, it should be underscored the high relative abundance of the genera *Mycobacterium*, *Bradyrhizobium* and acidobacterial *Gp6* and *Gp4*, which in sum accounted for >20 % of total sequences retrieved from the rhizosphere soils (both in NPD and NPH samples, Fig. 2A). Among them, just *Mycobacterium* and *Gp4* were differently abundant (ANCOM-BC, $p < 0.002$; Table S6); the first was significantly more represented in the rhizosphere of healthy trees, whilst *Gp4* followed the opposite trend (Fig. 2A). Other genera were also not equally distributed in the rhizosphere of both types of trees, although they were minor genera. Among them, genera *Bacillus*, *Neobacillus*, *Peribacillus* and *Cytobacillus* (family Bacillaceae_1) were more predominant in decline-affected trees (Table S6). Regarding the root endosphere, *Streptomyces* accounted for a higher percentage of sequences in symptomatic trees (20.4 ± 13.64 %) than in unaffected ones (7.8 ± 10.99 %, Fig. 2B), although this difference was not statistically significant (ANCOM-BC, $p = 1$) and camouflaged due to the high dispersion of the data. Another actinobacterial genus, *Micromonospora*, reigned the inner part of the roots of healthy trees, accounting for an outstanding percentage of sequences (*c.* 12 %; ANCOM-BC, $p = 1.7 \cdot 10^{-7}$; Fig. 2B). It should be emphasized that some genera were differentially abundant when comparing both types of trees, and they followed the same distribution pattern in the rhizosphere and in the root endosphere. This was the case of *Bacillus*, *Cytobacillus*, *Neobacillus*, *Peribacillus* (Family Bacillaceae_1), *Nonomuraea* and *Actinokineospora* (significantly more abundant in diseased trees; ANCOM- BC, $p < 0.049$; Table S6), and *Caballeronia* and *Derxia*, enriched in unaffected maritime pines. Interestingly enough, the abundance of the family Bacillaceae_1 increased significantly in diseased trees (ANCOM-BC, $p_{rhizosphere} = 2.41 \cdot 10^{-46}$, $p_{endosphere} = 6 \cdot 10^{-18}$) when comparing to healthy individuals.

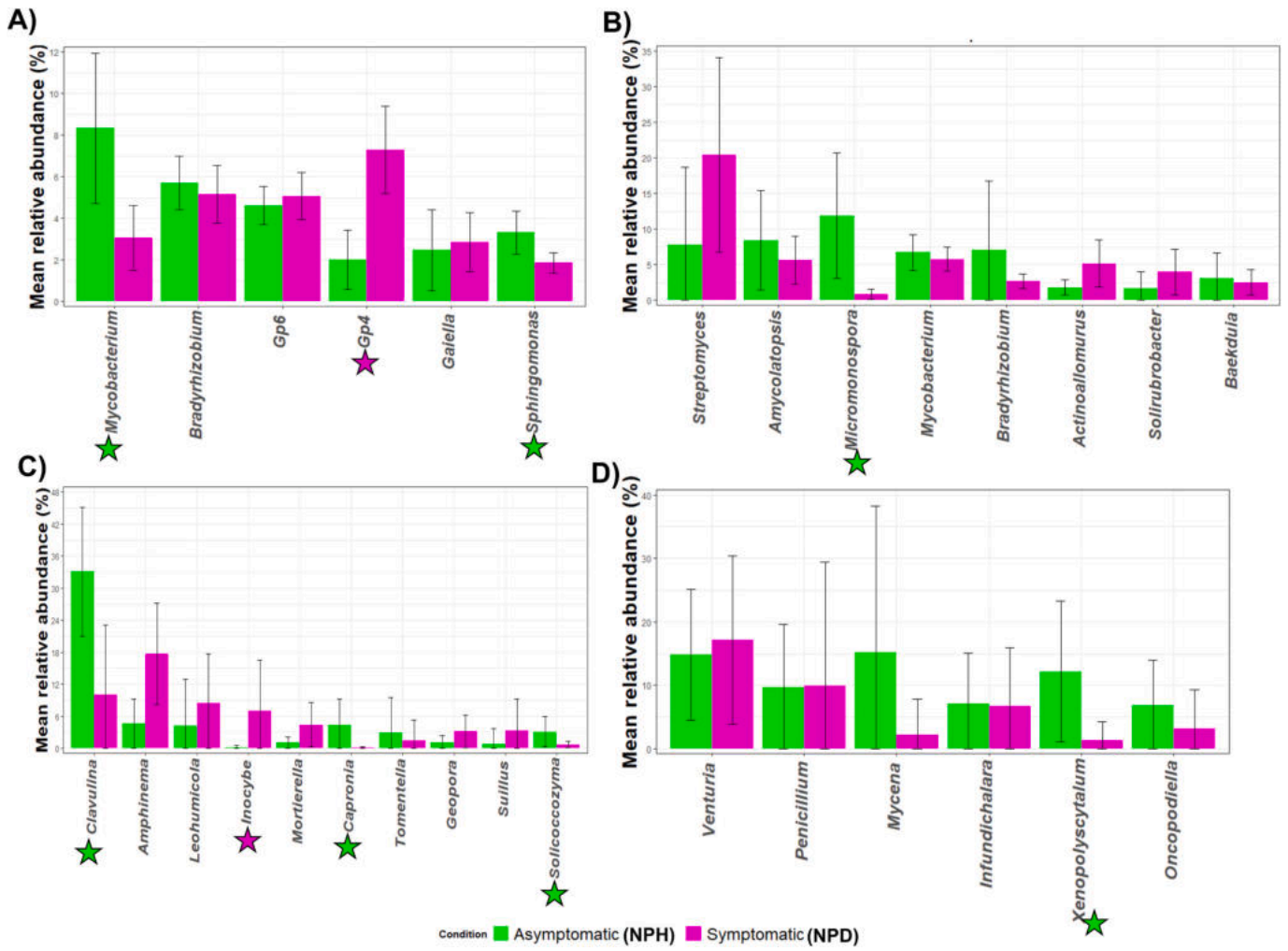

Fig. 2. Mean relative abundance of the main bacterial genera inhabiting the rhizosphere (A) and root endosphere (B) and fungal genera dwelling in the rhizosphere (C) and root endosphere (D) of healthy and decline-affected *P. pinaster* trees. Bars indicate the standard deviation of all the replicates. Just those genera accounting for most than 5 % of the total sequences of the corresponding dataset are shown. Green stars indicate genera significantly enriched in the corresponding compartment of asymptomatic trees (NPH), while pink stars represent genera significantly enriched in decline-affected trees (NPD) according to ANCOM-BC test.

Concerning the fungal communities, the rhizosphere of NPH and NPD trees were mainly dominated by *Clavulina* and *Amphinema*, which accounted >33 and 17 % of the total sequences, respectively (Fig. 2C). The former one, along with other abundant genera such as *Cladophialophora*, *Solicoccozyma*, *Knufia*, *Xenopolyscytalum* and *Capronia*, showed a significant increase in the rhizosphere of unaffected trees (ANCOM-BC, $p < 4.2 \cdot 10^{-4}$; Table S6). On the contrary, *Inocybe* and *Gymnopus* were more abundant in diseased than in healthy trees (Table S6). In the root endosphere, just 12 genera were differentially distributed in both types of trees. Among the most abundant genera (Fig. 2D), *Xenopolyscytalum* was significantly enriched in the endosphere of unaffected pines, according to ANCOM-BC results ($p = 6 \cdot 10^{-4}$). It should be noted that diseased trees showed more abundance of *Cadophora* and *Chrysosporium* than healthy trees in both rhizosphere and root endosphere, whilst the opposite trend was detected for *Capronia*, *Hyaloscypha*, *Phialochephala*, *Sagenomella*, *Xenopolyscytalum* and the ectomycorrhizal fungi (ECM) *Clavulina* and *Tylospora*. Indeed, the relative abundance of the group formed by fungal genera classified as ECMs was markedly higher in the root endosphere of NPH than in that of NPD pines (NPH: 7.9 %, NPD: 2.4 %; Yuen's *t*-test, $p = 0.037$, $\xi = 0.902$). No differences were identified in the abundance of ECM in the rhizosphere of NPD and NPH trees.

As summarized in Table S6, some potential pine pathogens such as the genera *Cadophora*, *Giberella* and *Mycosphaerella* were identified, being all of them more abundant in the endosphere and/or the rhizosphere of diseased trees, although the latter did not show statistically significant differences.

3.5. Uncovering the assembly of root-associated microbiota

Co-occurrence network analyses revealed that microbial communities assembled in a different way according to the health status of the pines; the same pattern was observed for both plant compartments. The root microbiota of healthy trees formed more compact and complex networks that of diseased individuals (Fig. S5, Fig. S6). These networks were comprised by a higher number of nodes and links and average degree (avgK), and the average cluster coefficient (avgCC) was significantly higher than in the networks of affected trees (Table 1). By contrast, the geodesic distance (GD) was significantly higher in the networks of diseased pines. Healthy and decline-affected trees also differed in the amount and taxonomy of the keystone members (Table S7). Fungal ASV01099 (belonging to the potentially pathogenic genus *Mycosphaerella*) was a peripheral node of the network corresponding to the endosphere of diseased trees.

3.6. Metabolic response to forest decline

Metabolic profiles of root and rhizosphere samples revealed significant differences in both plant compartments between healthy and

Table 1
Main topological properties of the microbial co-occurrence networks. Asterisk indicate significant differences in the corresponding parameters between NPD and NPH trees (Student's t-test, $p < 0.05$).

	Rhizosphere		Root endosphere	
	NPD	NPH	NPD	NPH
R^2 [a]	0.935	0.936	0.745	0.7
Nodes	223	281	114	129
Links	235	444	132	169
PEP[b] (%)	27.66	42.57	6.06	3.55
Centralization of stress centrality (Cs)	0.742*	7.201*	0.617	0.573
Average Degree (avgK)	2.108	3.16	2.316	2.62
Average Clustering Coefficient (avgCC)	0.006*	0.068*	0.026*	0.056*
Geodesic Distance (GD)	6.143*	5.569*	6.695*	5.876*
Modularity[c]	0.826 (37)	0.721 (36)	0.765 (13)	0.761 (15)

[a] R^2, R^2 of power law.
[b] *PEP*, Percentage of positive links.
[c] Modularity and the number of modules (in brackets).

decline-affected individuals. Notably, metabolites were universally detected across all samples, exhibiting quantitative variations associated with the health status of the trees.

A total of 299 distinct compounds were quantified in the roots of *P. pinaster* trees, 69 of which were successfully characterized, while the remaining 230 remained unidentified. Based on fold-change analysis, a total of 12 compounds were significantly enriched in the roots of symptomatic trees (log2FC $\geq$ 1.5; Table S8). Conversely, 30 compounds were significantly more abundant in healthy trees (Fig. 3A; Table S8). Additionally, metabolic pathways were analyzed in both tree types (Table S8). Pathways enriched in decline-affected trees were associated with arginine metabolism, primarily involving degradation processes, whereas pathways enriched in healthy trees were closely linked to flavonoid biosynthesis, particularly quercetins and their derivatives (Fig. 4).

Analysis of rhizosphere samples revealed 662 distinct compounds between symptomatic and asymptomatic trees, 368 of which were successfully identified. A total of 282 and 255 compounds were significantly enriched in the rhizosphere of healthy and decline-affected trees, respectively (log2FC $\geq$ 1.5; Fig. 3B; Table S9). Examination of metabolite profiles in the rhizosphere of both tree types (Table S9) highlighted differences in both primary and secondary metabolism. Forest decline-affected trees exhibited a notable upregulation of metabolites associated with defensive responses against biotic factors, highlighted by an accumulation of secondary metabolites, particularly flavonoids (Fig. 5; Table S9). On the contrary, healthy pines accumulated significantly more metabolites involved in primary metabolism such as lipids and organic acids in the rhizosphere (Fig. 5; Table S9).

Additionally, significant differences in phytohormone metabolism were observed between healthy and decline-affected individuals. While non-affected pines exhibited a notable accumulation of gibberellins and jasmonic acids, unhealthy trees were enriched in methyl gibberellins, which are related to gibberellin catabolic processes (Table S9).

3.7. Connecting the P. pinaster root microbiome with the metabolome

We uncovered the potential interactions between metabolites and microorganisms in both rhizosphere soils and roots. In the former, several compounds which were significantly more abundant in decline-affected trees correlated positively with ASV00055 (acidobacterial *Gp4*) and/or with ASV00618 (unclassified genus, family Spartobacteria; Fig. 6A). On the other hand, the metabolite Choline sulfate (significantly enriched in healthy trees) correlated positively with an ASV belonging to the genus *Caballeronia*. Regarding the roots, significant negative correlations were detected among aminoacids and their derivatives (which were differentially enriched in diseased plants) and the ASV00004 belonging to *Bradyrhizobium*. At the same time, this ASV correlated negatively with 5-Guanidino-2-oxopentanoate, a product of the deamination of L-arginine (Fig. 6B). Furthermore, an ASV belonging to *Amycolatopsis* genus stablished a positive correlation with the compound Phomalichenone D significantly more abundant in asymptomatic trees.

4. Discussion

Here we deciphered the composition of root microbial communities and metabolome of *P. pinaster* trees affected by decline in comparison to healthy individuals. Firstly, it should be underscored that the cause of the forest decline was not disentangled in the present study. We can neither confirm whether the infection by *Matsucoccus feytaudi* induced tree decline, nor rule out a weakening of the affected trees (by other unmeasured factors) prior to the infection by the insect. Moreover, the implication of other factors in *P. pinaster* decline such as the observed shifts in microbial communities, the potential pathogens here detected, or abiotic factors (i.e., soil organic matter, carbon:nitrogen ratio, percentage of sand and clay) can neither be validated nor ruled out.

Notwithstanding, we detected shifts in the alpha diversity and taxonomic profiles of bacterial and fungal communities when comparing both types of trees. Certain taxa previously found to be abundant in the rhizosphere or roots of healthy *Pinus* spp. individuals such as the bacterial genera *Micromonospora* (Li et al., 2014), *Mycobacterium* (Lasa et al., 2022a) or the fungal genera *Clavulina* (Harries, 2021; Wang et al., 2022) and *Xenopolyscytalum* (Zhao et al., 2020), among others, were significantly depleted in the rhizosphere soil or root endosphere of NPD (symptomatic) trees. These altered taxonomical profiles were accompanied by changes in the assembly pattern of root-associated microbial communities. Indeed, the co-occurrence networks of unaffected trees were more complex, tight and connected than that of diseased individuals. Our results are in accordance with those of Gómez-Aparicio et al. (2022), who found that the co-occurrence networks of decline-affected *Quercus suber* infected by the pathogen *Phytophthora cinnamomi* were less complex than that of healthy trees. Complex microbial networks are commonly linked to the suppression of plant diseases (Yang et al., 2017) and are expected to better cope with environmental disturbances (Berry and Widder, 2014), thus having an overall positive effect on the plant hosts (Tao et al., 2018; Wagg et al., 2019). Although we cannot decipher whether the increased complexity of the network calculated for the asymptomatic trees prevented them from being affected by forest decline, we can confirm that this phenomenon also alters the assembly of microbial communities. The one pathogen-one disease hypothesis is not enough to describe the disease processes in plants, according to Mannaa and Seo (2021). That out-dated appreciation is moving towards a more holistic paradigm, in which alterations in the structure coupled with changes in the assembly of balanced microbial communities might lead to destabilization of the microbiota, contributing to the development of disease symptoms. Although we cannot address the cause of pine decline here observed, our results demonstrate that symptomatic trees harbored altered microbial communities at different levels (diversity, taxonomical profiles and assembly patterns), which fits well with the disease model proposed by Mannaa and Seo (2021). On the other hand, it should be underscored that a significant increase in the abundance of the genera *Cadophora*, *Gibberella* and *Mycosphaerella* – for which pathogenic species affecting pine trees have been previously described (Friel et al., 2007; Chen et al., 2022a) – was detected for NPD trees. Further works should identify and characterize the potential involvement of these genera in forest decline.

We detected that several plant growth promoting microorganisms (PGPM) were enriched in the rhizosphere and/or root endosphere of decline-affected trees. Namely, *Streptomyces* (Viaene et al., 2016), several members of the family Bacillaceae_1, such as *Neobacillus*, *Peribacillus* and *Bacillus* (Rudrappa et al., 2008; Hernández-Pacheco et al., 2021; Peng et al., 2021) and certain *P. pinaster* ECM, for instance

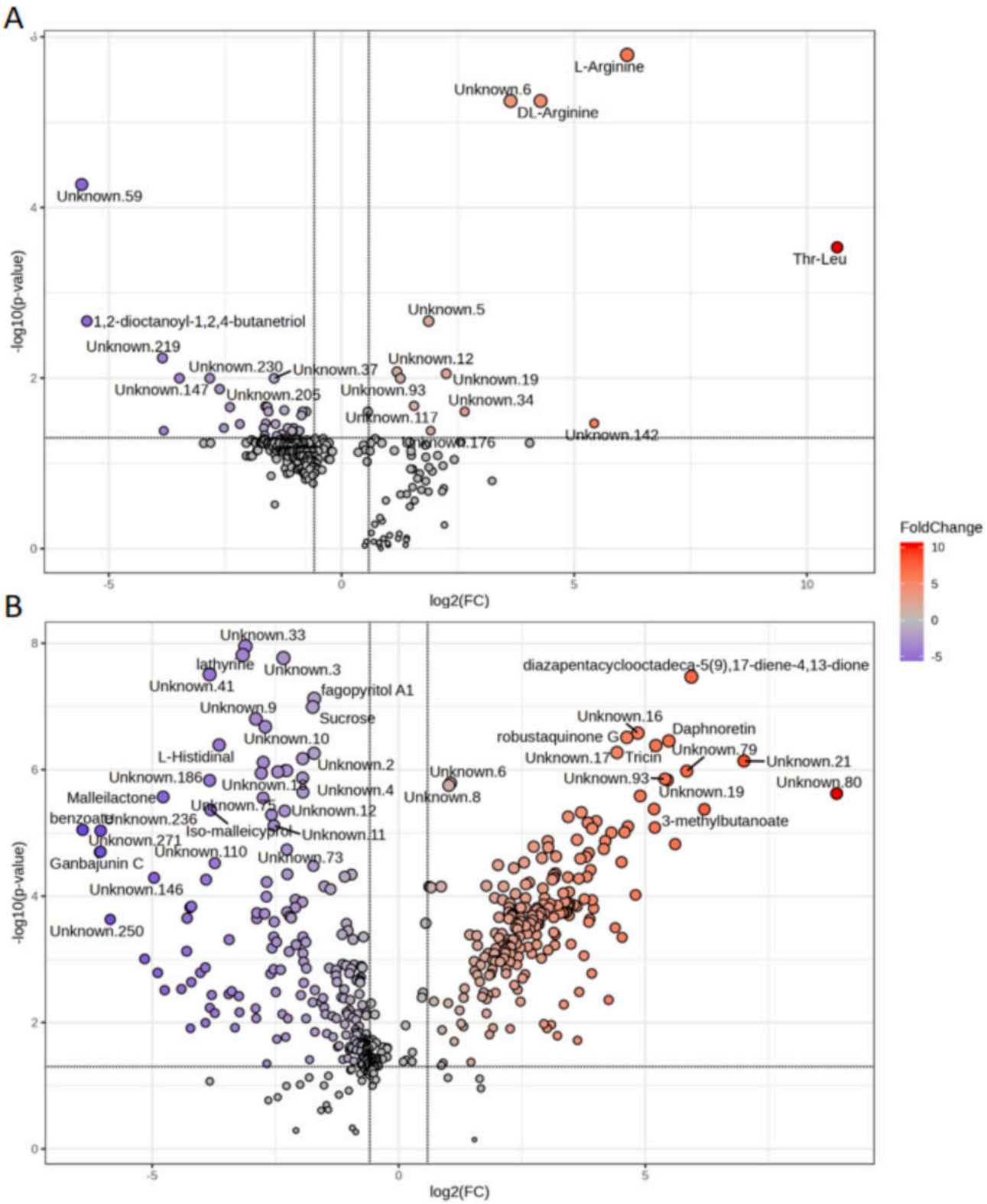

Fig. 3. Volcano plots of metabolic profiles comparing differentially abundant metabolites in (A) roots and (B) rhizosphere soil of decline-affected (NPD) and healthy (NPH) *P. pinaster* trees. Metabolites significantly more abundant in NPD trees are in red, while those significantly more abundant in NPH trees are in blue (Log2FC < -1.5 and Log2FC ≥ 1.5, respectively, $p < 0.05$). Metabolites that did not show significant differences between NPD and NPH trees are colored in grey. The list of metabolites is provided in Table S10.

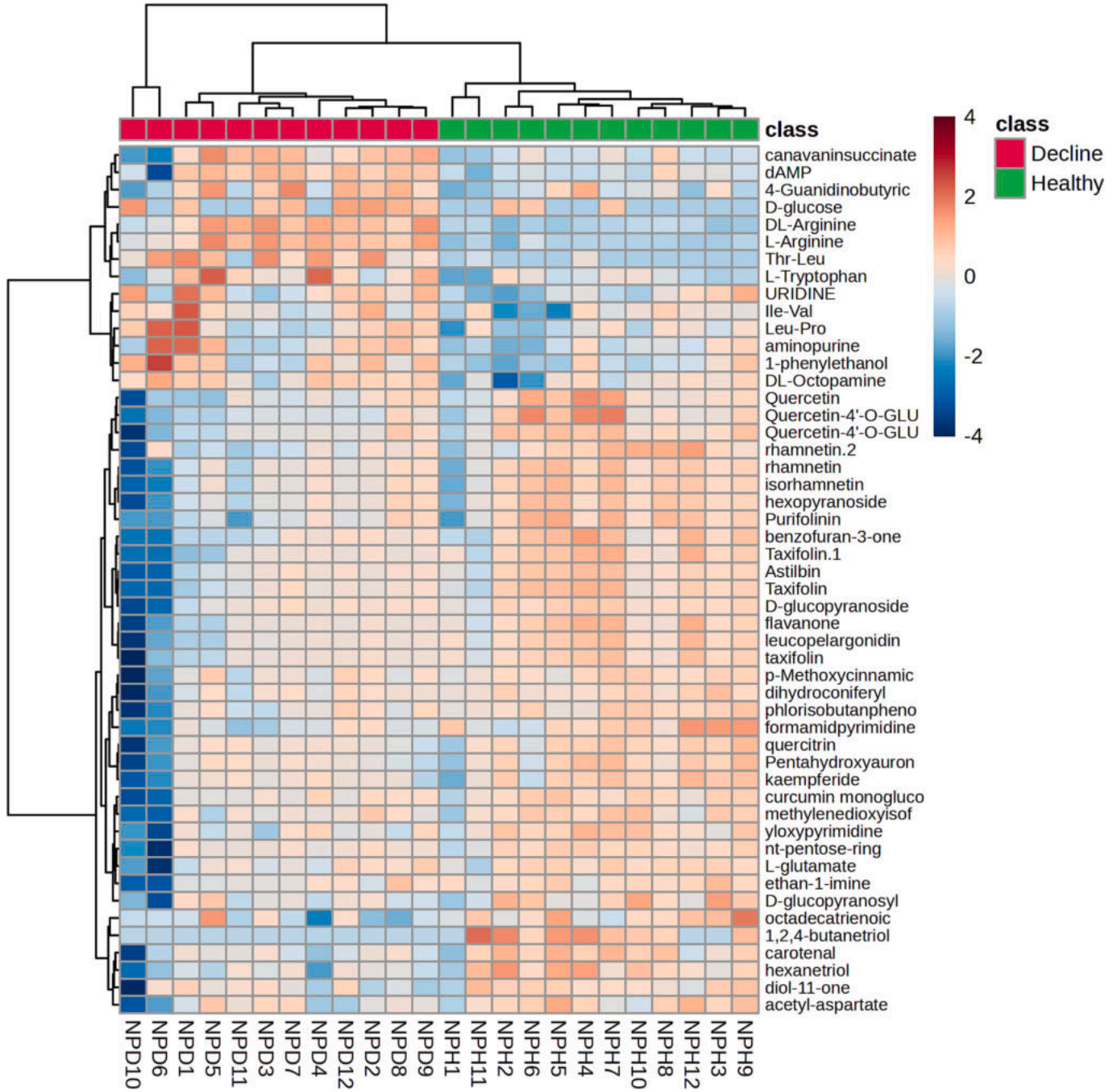

Fig. 4. Heat map derived from hierarchical clustering analysis of the metabolomics profile of root samples from healthy (NPH) and decline-affected (NPD) *P. pinaster* trees. Heatmap was obtained using normalized concentrations of the top 50 metabolites from *t*-test (Euclidean distance measure, Ward clustering method). The color code is presented on a logarithmic scale. List of the abbreviations is included in Table S10.

Anphinema and *Inocybe* (Castaño et al., 2018). All these results suggest that unhealthy trees may have recruited certain PGPM selectively as a consequence of the decline episode, thus, following a *cry-for-help* strategy. Growing body of works have demonstrated that even woody plants affected by pathogens, pests or other stresses can attract different beneficial microorganisms to alleviate the negative effects of the disturbances (Berendsen et al., 2018; Liu et al., 2021; Wu et al., 2021). However, it should be marked that potentially beneficial microorganisms were detected in the roots of both decline-affected and unaffected pines, suggesting a selective recruitment of specific microorganisms, probably mediated by different mechanisms or host metabolites.

The aboveground pest or pathogen infections may lead to alterations in the belowground microbiota (which is in line with our results), including the recruitment of plant beneficial microorganisms (Yuan et al., 2018; Rizaulin et al., 2021). This attraction or *cry-for-help* strategy is commonly mediated by the excretion of specific metabolites in the root exudates. The differences here observed in the root metabolic profiles between healthy and affected pine trees partially endorse the idea of a selective microbial recruitment by decline-affected trees. In the case of rhizosphere soil samples, an enrichment in defensive secondary metabolites mainly associated with the metabolism of tricines, myricetins, luteolins, and anthraquinones (Lam et al., 2021; Rong et al., 2023; Wang et al., 2023) was observed in affected trees, while in healthy individuals, there was a significantly greater accumulation of

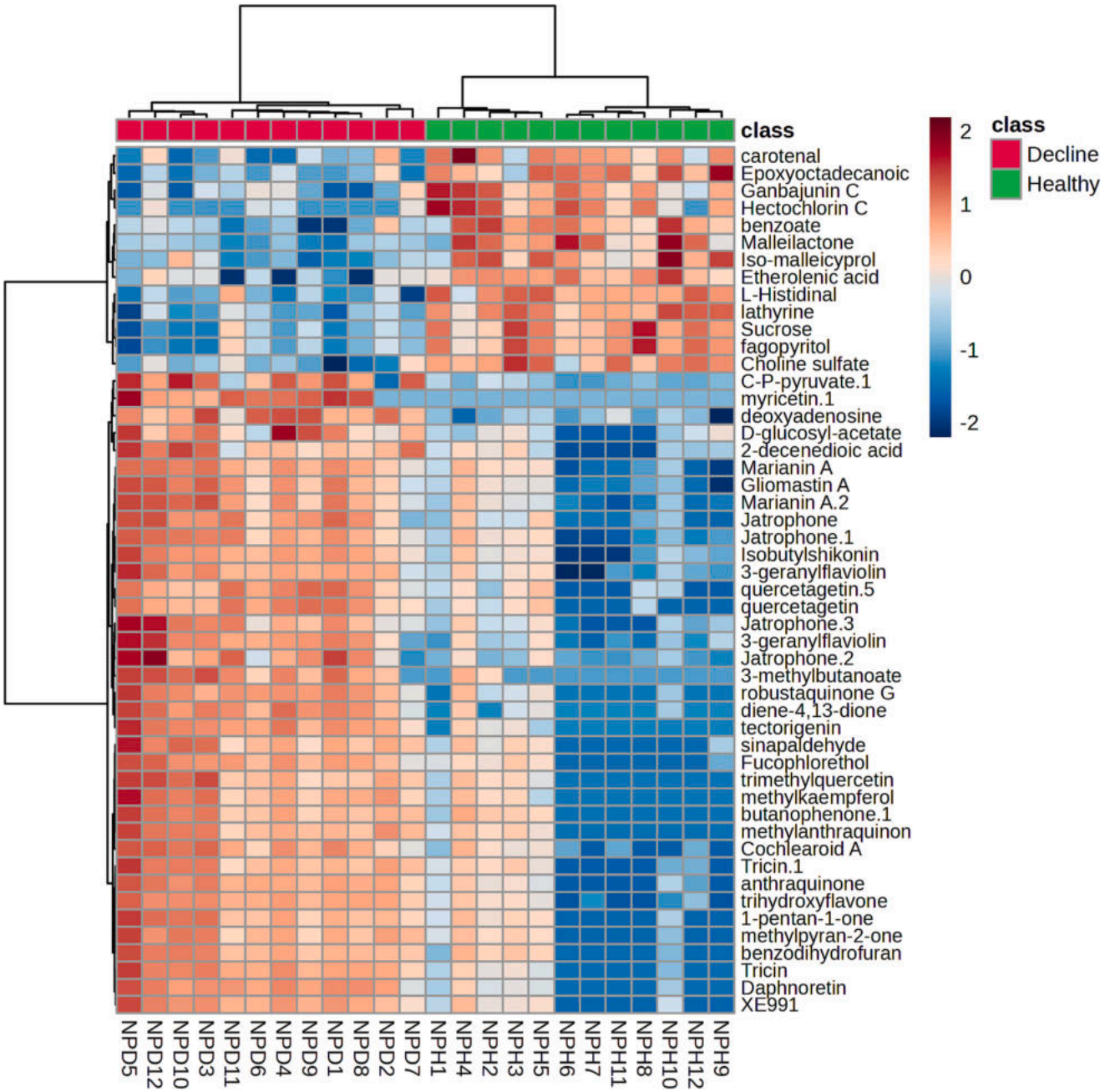

Fig. 5. Heat map derived from hierarchical clustering analysis of the metabolomics profile of rhizosphere samples from healthy (NPH) and decline-affected (NPD) *P. pinaster* trees. Heatmap was obtained using normalized concentrations of the top 50 metabolites from t-test (Euclidean distance measure, Ward clustering method). The color code is presented on a logarithmic scale. List of the abbreviations is included in Table S10.

compounds associated with primary metabolism. Some authors have reported that defensive secondary metabolites released by the plant roots upon an insect attack can recruit beneficial bacteria and fungi (reviewed by Rizaulin et al., 2021). On the other hand, differences were also recorded between the rhizosphere of both types of trees in the levels of regulatory phytohormones triggering plant defense. While multiple compounds related to the catabolism of gibberellins were identified in NPD trees, healthy plants showed an enrichment in compounds involved in gibberellin and jasmonic acid biosynthesis. Yuan et al. (2018) demonstrated that plants grown in preconditioned soils rich in jasmonic acid showed increased resistance levels against a bacterial phytopathogen.

We also detected significant correlations between microorganisms and metabolites, which could aid in deciphering potential microbial-plant interactions. For instance, we registered negative correlations between aminoacids and peptides enriched in affected plants, and the ASV00004 belonging to *Bradyrhizobium*, which also established a negative correlation with 5-Guanidino-2-oxopentanoate. That amino-acid derivative has previously been identified as a product of the deamination of L-Arg in *Pseudomonas aeruginosa* (Ohshima et al., 2022). Hence, ASV00004 could be involved somewhat in the L-Arg metabolism. It should be considered that *Bradyrhizobium* is an already known nitrogen fixing bacteria as well, thus, a member involved in the nitrogen cycle and in the metabolism of aminoacids. On the other hand, we detected a positive correlation between this ASV and Phomalichenone D (significantly enriched in healthy trees), and also between that metabolite and the ASV00043. Other phomalichenones are already known by their antibacterial activity in vitro (Chen et al., 2022b). Considering that

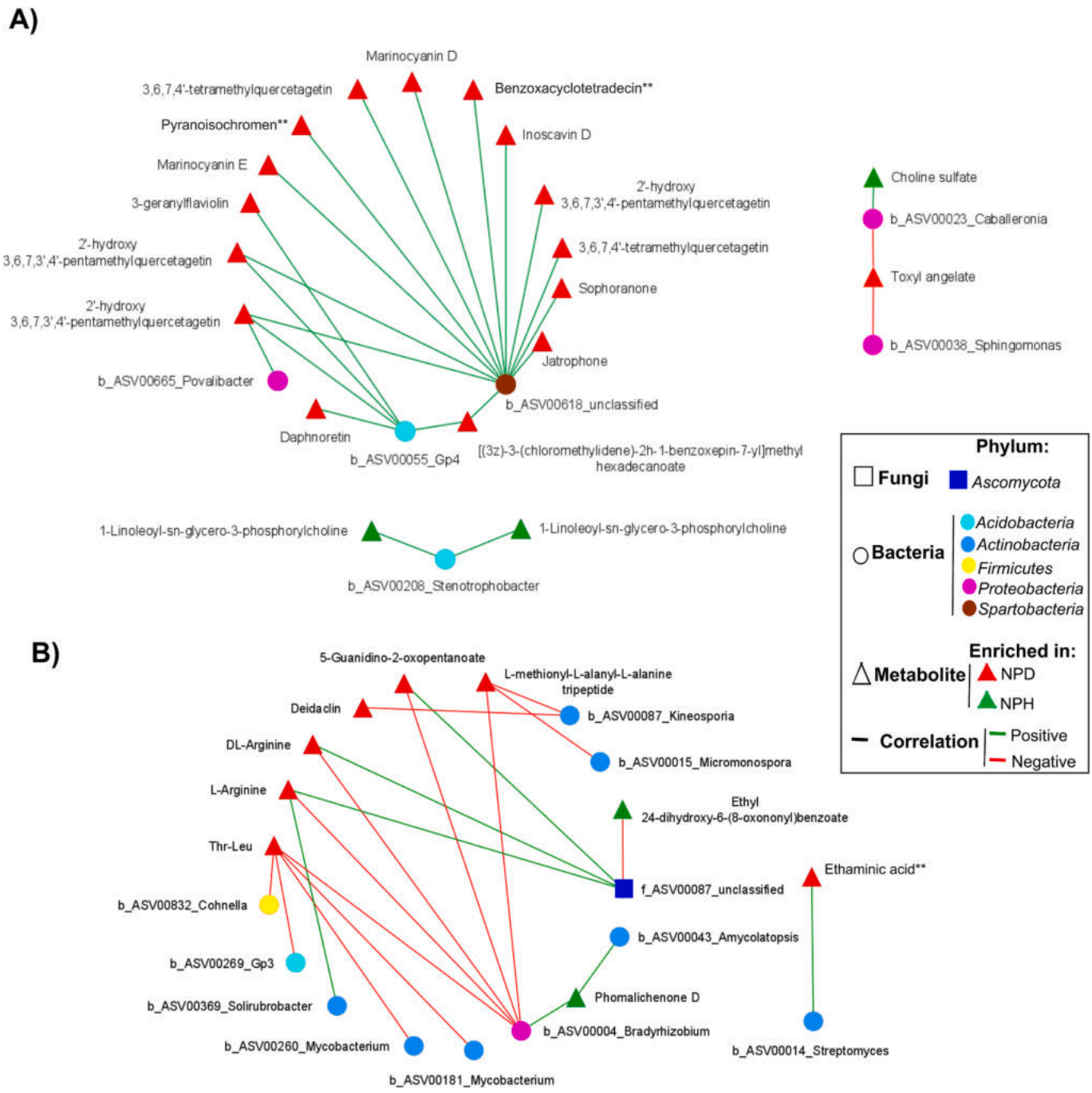

Fig. 6. Microorganisms-metabolites co-occurrence networks of rhizosphere soil (A) and root samples (B). Red and green lines indicate statistically significant negative and positive links, respectively, among fungi, bacteria and metabolites. *. Circles represent bacterial ASVs, square denotes a fungal ASV, and triangles represent metabolites. The colors of circles and square summarize the bacterial and fungal phyla to which the corresponding ASV belongs, respectively. The colors of the triangles indicate the condition of the tree in which the corresponding metabolite is enriched. NPD: *P. pinaster* trees affected by decline, NPH: unaffected trees. * Benzoxacyclotertradecin: 13-bromo-7,8,9,16-tetrahydroxy-14-methoxy-3-methyl-3,4,7,8,9,10-hexahydro-2-benzoxacyclotetradecin-1-one; **Pyranoisochromen: 3-[2-(3,4-dihydroxyphenyl)ethenyl]-8,9-dihydroxy-6-methoxy-6 h-pyrano[4,3-*c*]isochromen-1-one; **Ethaminic acid: n-(4,5-dihydroxy-2-{[1-hydroxy-1-(4-hydroxy-2-imino-5,6,7,8-tetrahydro-1 h-pteridin-6-yl)propan-2-y]oxy}-6-(hydroxymethyl)oxan-3-yl)ethaminidic acid.

the latter ASV belongs to the genus *Amycolatopsis* which is known for its prolific secondary metabolite production (many of them with antibacterial activities, Kisil et al., 2021), it may be involved in the biosynthesis of that inhibitory compound, and therefore, in the asymptomatic status of healthy trees. Notwithstanding, it is worth mentioning that positive correlations between two nodes just implies that the abundance of both of them increased in the same way, thus, the presence of that ASV may suppose an enrichment in the metabolite (or vice versa). In the same line of reasoning we suggest that the increase in the abundance of ASV000055 (Acidobacteria *Gp4*) and ASV00618 (class Spartobacteria) could ultimately entail an increase of many different compounds such as Marinocyanin D and E, Inoscavin D, derivatives of quercetagetins and Daphnoretin in the rhizosphere of unhealthy pines, for which antimicrobial effect have already been described (Cottigli et al., 2001; Asolkar et al., 2017; Avigliano et al., 2019). Although we cannot decipher whether these metabolites were produced by both bacteria or excreted by the plant, their role in the plant defense against stresses should be studied in the future.

Overall, our results show not only that pine decline and/or the insect attack have a clear effect on the root microbiome and metabolic profiles but also shed light on the mechanisms underlying plant response. We cannot unravel the specific involvement of the microorganisms that are significantly correlated with differentially enriched metabolites, however, here we lay the groundwork for the microorganisms that could be important in the response to *P. pinaster* decline. Furthermore, our results demonstrate that this phenomenon should be looked at from a holistic perspective, including both tree-associated microbiota and the metabolome. More research is needed to corroborate whether the results here obtained are common in other forests worldwide subjected to different environmental conditions and applicable to other pine species.

Supplementary data to this article can be found online at https://doi.org/10.1016/j.scitotenv.2025.178486.

CRediT authorship contribution statement

Ana V. Lasa: Writing – review & editing, Writing – original draft, Visualization, Validation, Software, Methodology, Investigation, Formal analysis, Data curation, Conceptualization. **Miriam López-Hinojosa:** Writing – review & editing, Writing – original draft, Visualization, Validation, Software, Methodology, Investigation, Formal analysis, Data curation. **Pablo J. Villadas:** Writing – review & editing, Methodology, Conceptualization. **Antonio José Fernández-González:** Writing – review & editing, Methodology, Conceptualization. **María Teresa Cervera:** Writing – review & editing. **Manuel Fernández-López:** Writing – review & editing, Supervision, Project administration, Methodology, Funding acquisition, Conceptualization.

Funding

This work was supported by the MICINN through European Regional Development Fund [SUMHAL, LIFEWATCH-2019-09-CSIC-13, POPE 2014–2020].

Declaration of competing interest

The authors declare no competing financial interest or personal relationships that could have influenced the work reported in this paper.

Data availability

The microbiota and metabolomics datasets generated in the current study are deposited and available at the National Center for Biotechnology Information Sequence Read Archive (NCBI SRA) repository under the BioProject PRJNA1089945 (https://www.ncbi.nlm.nih.gov/bioproject/?term=(PRJNA1089945), and at the Open Society Foundations (OSF) repository under the project linked at https://osf.io/7vwc2/?view_only=9fb87740dd43406a9c76b046c44f1ae2, respectively.

References

Abarenkov, K., Zirk, A., Piirmann, T., Pöhönen, R., Ivanov, F., et al., 2022. UNITE general FASTA release for eukaryotes. v7.2 (version 7.2).

Ali, E., Cramer, W., Carnicer, J., Georgopoulou, E., Hilmi, N.J.M., et al., 2022. Cross-chapter paper 4: Mediterranean region. In: Pörtner, H.O., Roberts, D.C., Tignor, M., Poloczanska, E.S., Mintenbeck, K., et al. (Eds.), Climate Change 2022: Impacts, Adaptation and Vulnerability. Contribution of Working Group II to the Sixth Assessment Report of the Intergovernmental Panel on Climate Change. Cambridge University Press, Cambridge and New York, pp. 2233–2272.

Allen, C.D., Macalady, A.K., Chenchouni, H., Bachelet, D., McDowell, N., et al., 2010. A global overview of drought and heat-induced tree mortality reveals emerging climate change risks for forests. For. Ecol. Manage. 29, 660–684. https://doi.org/10.1016/j.foreco.2009.09.001.

Álvarez, G., Fernández, M., Diez, J.J., 2015. *Ophiosyomatoid* fungi associated with declined *Pinus pinaster* stands in Spain. For. Sys. 24, e006. https://doi.org/10.5424/fs/2015241-05707.

Asolkar, R.N., Singh, A., Jensen, P.R., Aalbersberg, W., Carté, B.K., et al., 2017. Marinocyanins, cytotoxic bromo-phenazinone meroterpenoids from a marine bacterium from the streptomycete clade MAR4. Tetrahedron 73, 2234–2241. https://doi.org/10.1016/j.tet.2017.03.003.

Avigliano, E., Rosso, J.J., Litjmaer, D., Ondarza, P., Piacentini, L., et al., 2019. Biodiversity and threats in non-protected areas: a multidisciplinary and multi-taxa approach focused on the Atlantic Forest. Helyon 5, E02292. https://doi.org/10.1016/j.heliyon.2019.e02292.

Azcárate, F.M., Seoane, J., Silvestre, M., 2023. Factor affecting pine processionary moth (*Thaumetopoea pityocampa*) incidence in Mediterranean pine stands: a multiscale approach. For. Ecol. Manage. 529, 120728. https://doi.org/10.1016/j.foreco.2022.120728.

Berendsen, R.L., Vismans, G., Yu, K., Song, Y., De Jonge, R., et al., 2018. Disease induced assemblage of a plant-beneficial bacterial consortium. ISME J. 12, 1496–1507. https://doi.org/10.1038/s41396-018-0093-1.

Berry, D., Widder, S., 2014. Deciphering microbial interactions and detecting keystone species with co-occurrence networks. Front. Microbiol. 5, 219. https://doi.org/10.3389/fmicb.2014.00219.

Bonini, P., Kind, T., Tsugawa, H., Barupal, D.K., Fiehn, O., 2020. Retip: retention time prediction for compound annotation in untargeted metabolomics. Anal. Chem. 92, 7515–7522. https://doi.org/10.1021/acs.analchem.9b05765.

Calama, R., Martínez, C., Gordo, J., del Río, M., Menéndez-Miguélez, M., 2024. The impact of climate and management on recent mortality in *Pinus pinaster* resin-tapped forests of inland Spain. Forestry: An International Journal of Forest Research 97, 1020–1132. https://doi.org/10.1093/forestry/cpad023.

Callahan, B.J., McMurdie, P.J., Rosen, M.J., Han, A.W., Johnson, A.J.A., et al., 2016. DADA2: high-resolution simple inference from Illumina amplicon data. Nat. Methods 13, 581–583. https://doi.org/10.1038/nmeth.3869.

Calvão, T., Duarte, C., Pimentel, C.S., 2019. Climate and landscape patterns of pine forest decline after invasion by the pinewood nematode. For. Ecol. Manage. 433, 43–51. https://doi.org/10.1016/j.foreco.2018.10.039.

Carnicer, F., Coll, M., Ninyerola, M., Pons, X., Sánchez, G., Peñuelas, J., 2011. Widespread crown condition decline, food web disruption, and amplified tree mortality with increased climate change-type drought. Proc. Natl. Acad. Sci. U. S. A. 108, 1474–1478. https://doi.org/10.1073/pnas.1010070108.

Castaño, C., Alday, J.G., Lindahl, B.D., Martínez de Aragón, J., de Miguel, S., et al., 2018. Lack of thinning effects over inter-annual changes in soil fungal community and diversity in a Mediterranean pine forest. For. Ecol. Manage. 424, 420–427. https://doi.org/10.1016/j.foreco.2018.05.004.

Chen, Q., Bakhshi, M., Balci, Y., Broders, K.D., Cheewangkoon, R., et al., 2022a. Genera of phytopathogenicfungi: GOPHY 4. Stud. Mycol. 101, 417–564. https://doi.org/10.3114/sim.2022.101.06.

Chen, Y., Pang, X., He, Y., Lin, X., Zhou, X., et al., 2022b. Secondary metabolites from coral-associated fungi: source, chemistry and bioactivities. J. Fungi. 8, 1043. https://doi.org/10.3390/jof8101043.

Chong, J., Soufan, O., Li, C., Caraus, I., Li, S., et al., 2018. MetaboAnalyst 4.0: towards more transparent and integrative metabolomics analysis. Nucleic Acids Res. 46, 486–494. https://doi.org/10.1093/nar/gky310.

Cohen, J., 1988. Statistical Power Analysis for the Behavioral Sciences. Routledge Academic, New York.

Cole, J.R., Wang, Q., Fish, J.A., Chai, B., McGarrell, D.M., et al., 2014. Ribosomal database project: data and tools for high throughput rRNA analysis. Nucleic Acids Res. 42, 633–642. https://doi.org/10.1093/nar/gkt1244.

Cottigli, F., Loy, G., Garau, D., Floris, D., Caus, M., et al., 2001. Antimicrobial evaluation of coumarins and flavonoids from the stems of *Daphne gnidium* L. Phytomedicine 8, 302–305. https://doi.org/10.1078/0944-7113-00036.

Coyle, D.R., Klepzig, K.D., Koch, F.H., Morris, L.A., Nowak, J.T., et al., 2015. A review of southern pine decline in North America. For. Ecol. Manage. 349, 134–148. https://doi.org/10.1016/j.foreco.2015.04.007.

Dove, N.C., Carrell, A.A., Engle, N.L., Klingeman, D.M., Rodriguez, M., et al., 2022. Relationships between *Sphaerulina musiva* infection and the *Populus* microbiome and metabolome. mSystems 7. https://doi.org/10.1128/msystems.00120-22 e00120–22.

Fernández-González, A.J., Cardoni, M., Gómez-Lama Cabanás, C., Valverde-Corredor, A., Villadas, P.J., et al., 2020. Linking belowground microbial network changes to different tolerance level towards Verticillium wilt of olive. Microbiome 8, 11. https://doi.org/10.1186/s40168-020-0787-2.

Friel, C.J., Desjardins, A.E., Kirkpatrick, S.C., Gordon, T.R., 2007. Evidence for recombination and segregation of virulence to pine in a hybrid cross between *Gibberella circinata* and *G. subglutinans*. Mycol. Res. 111, 827–831. https://doi.org/10.1016/j.mycres.2007.05.004.

Gea-Izquierdo, G., Férriz, M., García-Garrido, M., Aguín, O., Elvira-Recuenco, M., et al., 2019. Synergistic abiotic and biotic stressors explain widespread decline of *Pinus pinaster* in a mixed forest. Sci. Total Environ. 685, 963–975. https://doi.org/10.1016/j.scitotenv.2019.05.378.

Gómez-Aparicio, L., Domínguez- Begines, J., Villa-Sanabria, E., García, L.V., Muñoz-Pajares, A.J., 2022. Tree decline and mortality following pathogen invasion alters the diversity, composition and network structure of the soil microbiome. Soil. Biol. Bioch. 166, 108560. https://doi.org/10.1016/j.soilbio.2022.108560.

Guzmán Álvarez, J.R., Gómez de Dios, M.A., Muñoz Risueño, A., Alguacil Picón, F., Gómez Milán, F., et al., 2020. The rol of *Matsucoccus feytaudi* Duc., 1941 influencing *Pinus pinaster* Ait. decline in the Natural Park of Sierra de Baza (Granada, Andalusia, Spain). Cuadernos de la Sociedad Española de Ciencias Forestales 46, 83–102. https://doi.org/10.31167/csecfv0i46.19903.

Harries, D., 2021. DNA barcoding reveals *Clavulina etruriae* - new to Britain. Field. Mycol. 22, 47–49. https://doi.org/10.1016/j.fldmyc.2021.04.007.

Hernández-Pacheco, C.E., Orozco-Mosqueda, M.C., Flores, A., Valencia-Cantero, E., Santoyo, G., 2021. Tissue-specific diversity of bacterial endophytes in Mexican husk tomato plants (*Physalis ixocarpa* Brot. Ex Horm.), and screening for their multiple

plant growth-promoting activities. Curr. Res. Microb. Sci. 2, 100028. https://doi.org/10.1016/j.crmicr.2021.100028.
Ihrmark, K., Bödeker, I.T.M., Cruz-Martinez, K., Friberg, H., Kubartova, A., et al., 2012. New primers to amplify the fungal ITS2 region – evaluation by 454- sequencing of artificial and natural communities. FEMS Microbiol. Ecol. 82, 666–677. https://doi.org/10.1111/j.1574-6941.2012.01437.x.
Kassambara, A., 2022. Rstatix: pipe-friendly framework for basic statistical tests. https://CRAN.R-project.org/package=rstatix.
Kisil, O.V., Efimenko, T.A., Efremenkova, O.V., 2021. Looking back to *Amycolatopsis*: history of the antibiotic discovery and future prospects. Antibiotics 10, 1254. https://doi.org/10.3390/antibiotics10101254.
Lam, P.Y., Lui, A.C.W., Wang, L., Liu, H., Umezawa, T., et al., 2021. Tricin biosynthesis and bioengineering. Front. Plant Sci. 12, 733198. https://doi.org/10.3389/fpls.2021.733198.
Lasa, A.V., Guevara, M.A., Villadas, P.J., Fernández-González, A.J., Cervera, M.T., et al., 2022a. Bacteriome dataset from the rhizosphere of trees in a *Pinus pinaster* and *Pinus halepensis* dominated forest subjected to drought conditions. Data Brief 46, 108805. https://doi.org/10.1016/j.dib.2022.108805.
Lasa, A.V., Guevara, M.A., Villadas, P.J., Vélez, M.D., Fernández-González, A.J., et al., 2022b. Correlating the above- and belowground genotype of *Pinus pinaster* trees and rhizosphere bacterial communities under drought conditions. Sci. Total Environ. 832, 155007. https://doi.org/10.1016/j.scitotenv.2022.155007.
Lasa, A.V., Fernández-González, A.J., Villadas, P.J., Mercado-Blanco, J., Pérez-Luque, A.J., et al., 2024. Mediterranean pine forest decline: a matter of root-associated microbiota and climate change. Sci. Total Environ. 926, 171858. https://doi.org/10.1016/j.scitotenv.2024.171858.
Li, C., Liu, C., Zhao, J., Zhang, Y., Gao, R., et al., 2014. *Micromonospora maoerensis* sp. nov., isolated from a Chinese pine forest soil. Antonie Van Leeuwenhoek 105, 9. https://doi.org/10.1007/s10482-013-0096-x.
Lin, H., Peddada, S.D., 2020. Analysis of compositions of microbiomes with bias correction. Nat. Commun. 11, 3514. https://doi.org/10.1038/s41467-020-17041-7.
Liu, H., Li, J., Carvalhais, L.C., Percy, C.D., Prakash Verma, J., et al., 2021. Evidence for the plant recruitment of beneficial microbes to suppress soil-borne pathogens. New Phytol. 229, 2873–2885. https://doi.org/10.1111/nph.17057.
López-Hidalgo, C., Lamelas, L., Cañal, M.J., Valledor, L., Meijón, M., 2023. Untarget metabolomics revealed essential biochemical rearrangements towards combined heat and drought stress acclimatization in *Pinus pinaster*. Environ. Exp. Bot. 20, 105261. https://doi.org/10.1016/j.envexpbot.2023.105261.
López-Hinojosa, M., de María, N., Guevara, M.A., Vélez, M.D., Cabezas, J.A., et al., 2021. Rootstock effects on scion gene expression in maritime pine. Sci. Rep. 11, 11582. https://doi.org/10.1038/s41598-021-90672-y.
Lundberg, D.S., Yourstone, S., Mieczkowski, P., Jones, C.D., Dangl, J.L., 2013. Practical innovations for high-throughput amplicon sequencing. Nat. Methods 10, 999–1002. https://doi.org/10.1038/nmeth.2634.
Madrigal-González, J., Zavala, M.A., 2014. Competition and tree age modulated last century pine growth responses to high frequency of dry years in a water limited forest ecosystem. Agric. For. Meteorol. 192-193, 18–26. https://doi.org/10.1016/j.agrformet.2014.02.011.
Mair, P., Wilcox, R., 2020. Robust statistical methods in R using the WRS2 package. Behav. Res. Methods 52, 464–488. https://doi.org/10.3758/s13428-019-01246-w.
Manion, P.D., 1991. Tree Disease Concepts, second ed. Prentice Hall Inc., Upper Saddle River.
Manjarrez, L.F., Guevara, M.Á., de María, N., Vélez, M.D., Cobo-Simón, I., et al., 2024. Maritime pine rootstock genotype modulates gene expression associated with stress tolerance in grafted stems. Plants 13, 1644. https://doi.org/10.3390/plants13121644.
Mannaa, M., Seo, Y.S., 2021. Plants under the attack of allies: moving towards the plant pathobiome paradigm. Plants 10, 125. https://doi.org/10.3390/plants10010125.
de María, N., Guevara, M.A., Perdiguero, P., Vélez, M.D., Cabezas, J.A., et al., 2020. Molecular study of drought response in the Mediterranean conifer *Pinus pinaster* Ait.: differential transcriptomic profiling reveals constitutive water deficit-independent drought tolerance mechanisms. Ecol. Evol. 10, 9788–9807. https://doi.org/10.1002/ece3.6613.
Martin, M., 2011. Cutadapt removes adapter sequences from high-throughput sequencing reads. EMBnet J. 17, 10–12. https://doi.org/10.14806/ej.17.1.200.
McMurdie, P.J., Holmes, S., 2013. Phyloseq: an R package for reproducible interactive analysis and graphics of microbiome census data. PloS One 8, e61217. https://doi.org/10.1371/journal.pone.0061217.
McMurdie, P.J., Holmes, S., 2014. Waste not, want not: why rarefying microbiome data is inadmissible. PLoS Comput. Biol. 10, e1003531. https://doi.org/10.1371/journal.pcbi.1003531.
Ohshima, T., Tanaka, M., Ohmori, T., 2022. $NADP^+$-dependent l-arginine dehydrogenase from *Pseudomonas velonii*: purification, characterization and application to an l-arginine assay. Protein Expr. Purif. 199, 106135. https://doi.org/10.1016/j.pep.2022.106135.
Oksanen, J., Simpson, G., Blanchet, F., Kindt, R., Legendre, P., et al., 2022. vegan: Community Ecology Package. R package version 2.6-2. https://CRAN.R-project.org/package=vegan.
Olesen, J.M., Bascompte, J., Dupont, Y.L., Jordano, P., 2017. The modularity of pollination networks. Proc. Natl. Acad. Sci. U. S. A. 104, 19891–19896. https://doi.org/10.1073/pnas.0706375104.
Peng, J., Ma, J., Wei, X., Zhang, C., Jia, N., et al., 2021. Accumulation of beneficial bacteria in the rhizosphere of maize (*Zea mays L.*) grown in a saline soil in responding to a consortium of plant growth promoting rhizobacteria. Ann. Microbiol. 71, 40. https://doi.org/10.1186/s13213-021-01650-8.
Prieto-Recio, C., Martín-García, J., Bravo, F., Diez, J.J., 2015. Unravelling the associations between climate, soil properties and forest management in *Pinus pinaster* decline in the Iberian Peninsula. For. Ecol. Manage. 356, 74–83. https://doi.org/10.1016/j.foreco.2015.07.033.
Proença, D.N., Francisco, R., Kublik, S., Schöler, A., Vestergaard, G., et al., 2017. The microbiome of endophytic, wood colonizing bacteria from pine trees as affected by pine wilt disease. Sci. Rep. 7, 4205. https://doi.org/10.1038/s41598-017-04141-6.
R Core Team, 2022. R: A language and environment for statistical computing. https://www.R-project.org/.
Riquelme, S., Campos, J.V., Alzamora, R., Fiehn, O., Pérez, A.J., 2023. Lipidomics analysis reveals the effect of *Sirex noctilio* infestation on the lipid metabolism in *Pinus radiate* needles. Plant Sci. 33, 111858. https://doi.org/10.1016/j.plantsci.2023.111858.
Rizaulin, M.S., Stopnisek, N., Raaijmarkers, J.M., Garbeva, P., 2021. The chemistry of stress: understanding the 'cry for help' of plant roots. Metabolites 11, 357. https://doi.org/10.3390/metabo11060357.
Robinson, M.D., McCarthy, D.J., Smyth, G.K., 2010. edgeR: a Bioconductor package for differential expression analysis of digital gene expression data. Bioinformatics 26, 139–140. https://doi.org/10.1093/bioinformatics/btp616.
Rong, J., Fu, F., Han, C., Wu, Y., Xia, Q., et al., 2023. Tectorigenin: a review of its sources, pharmacology, toxicity, and pharmacokinetics. Molecules 28, 5904. https://doi.org/10.3390/molecules28155904.
Rudrappa, T., Czymmek, K.J., Paré, P.W., Bais, H.P., 2008. Root-secreted malic acid recruits beneficial soil bacteria. Plant Physiol. 148, 1547–1556. https://doi.org/10.1104/pp.108.127613.
Russel, J., 2023. MicEco: various functions for microbial community data. R package version 0.9.19.
Sasada, R., Weinstein, M., Prem, A., Jin, M., Bhasin, J., 2020. FIGARO: an efficient and objective tool for optimizing microbiome rRNA gene trimming parameters. J. Biomol. Tech. 31, S2. https://doi.org/10.1101/610394.
Seybold, H., Demetrowitsch, T.J., Hassani, M.A., Szymczak, S., Reim, E., et al., 2020. A fungal pathogen induces systemic susceptibility and systemic shifts in wheat metabolome and microbiome composition. Nat. Commun. 11, 190. https://doi.org/10.1038/s41467-020-15633-x.
Shannon, P., Markiel, A., Ozier, O., Baliga, N.S., Wang, J.T., et al., 2003. Cytoscape: a software environment for integrated models of biomolecular interaction networks. Genome Res. 13, 2498–2504. https://doi.org/10.1101/gr.1239303.
Signorell, A., Aho, K., Alfons, A., Anderegg, N., Aragon, T., et al., 2022. DescTools: tools for descriptive statistics. https://cran.r-project.org/package=DescTools.
Spanish Ministry for Ecological Transition and the Demographic Challenge, 2024. https://www.miteco.gob.es/es/biodiversidad/temas/inventarios-nacionales/inventario-forestal-nacional/index.html. Last accessed: 26/02/2024.
Takahashi, S., Tomita, J., Nishioka, K., Hisada, T., Nishijima, M., 2014. Development of a prokaryotic universal primer for simultaneous analysis of bacteria and archaea using next-generation sequencing. PloS One 9, 8. https://doi.org/10.1371/journal.pone.0105592.
Tao, J., Meng, D., Qin, C., Liu, X., Liang, Y., et al., 2018. Integrated network analysis reveals the importance of microbial interactions for maize growth. Environ. Microbiol. 102, 3805–3818. https://doi.org/10.1007/s00253-018-8837-4.
Trivedi, P., Leach, J.E., Tringe, S.G., Sa, T., Singh, B.K., 2020. Plant-microbiome interactions: from community assembly to plant health. Nature Reviews 18, 607–621. https://doi.org/10.1038/s41579-020-0412-1.
Viaene, T., Langendries, S., Beirinckx, S., Maes, M., Goormachtig, S., 2016. *Streptomyces* as plant's best friend? FEMS Microbiol. Ecol. 92, fiw119. https://doi.org/10.1093/femsec/fiw119.
Wagg, C., Schlaeppi, K., Banerjee, S., Kuramae, E.E., van der Heijden, M.G.A., 2019. Fungal-bacterial diversity and microbiome complexity predict ecosystem functioning. Nat. Commun. 10, 4841. https://doi.org/10.1038/s41467-019-12798-y.
Wang, J., Han, S., Wang, C., Li, M.H., 2022. Long-term nitrogen-addition-induced shifts in the ectomycorrhizal fungal community are associated with changes in fine root traits and soil properties in a mixed *Pinus koraiensis* forest. Eur. J. Soil Biol. 112, 103431. https://doi.org/10.1016/j.ejsobi.2022.103431.
Wang, P., Wei, J., Hua, X., Dong, G., Dziedzic, K., et al., 2023. Plant anthraquinones: classification, distribution, biosynthesis, and regulation. J. Cell. Physiol. 31063. https://doi.org/10.1002/jcp.31063.
White, T.J., Bruns, T.D., Lee, S.B., Taylor, J.W., 1990. Amplification and direct sequencing of fungal ribosomal RNA genes for phylogenetics. In: Innis, M.A., Gelfand, D.H., Sninsky, J.J., White, T.J. (Eds.), PCR Protocols: A Guide to Methods and Applications. Academics Press, San Diego, pp. 315–322.
Wu, C., Wang, F., Ge, A., Zhang, H., Chen, G., et al., 2021. Enrichment of microbial taxa after the onset of wheat yellow mosaic disease. Agric. Ecosyst. Environ. 322, 107651. https://doi.org/10.1016/j.agee.2021.107651.
Yang, H., Li, J., Xiao, Y., Gu, Y., Liu, H., et al., 2017. An integrated insight into the relationship between soil microbial community and tobacco bacterial wilt disease. Front. Microbiol. 8, 2179. https://doi.org/10.3389/fmicb.2017.02179.
Yuan, J., Zhao, J., Wen, T., Zhao, M., Li, R., et al., 2018. Root exudates drive the soil-borne legacy of aboveground pathogen infection. Microbiome 6, 156. https://doi.org/10.1186/s40168-018-0537-x.
Zhao, P.S., Guo, M.S., Gao, G.L., Zhang, Y., Ding, G.D., et al., 2020. Community structure and functional group of root-associated Fungi of *Pinus sylvestris* var. *mongolica* across stand ages in the Mu Us Desert. Ecol. Evol. 10, 3032–3042. https://doi.org/10.1002/ece3.6119.